Published in final edited form as:
Radiat Res. 2011 May ; 175(5): 610–621. doi:10.1667/RR2297.1.

Oxidative Lipidomics of γ-Radiation-Induced Lung Injury: Mass Spectrometric Characterization of Cardiolipin and Phosphatidylserine Peroxidation

Yulia Y. Tyurina[a,b,1], **Vladimir A. Tyurin**[a,b], **Valentyna I. Kapralova**[a,b], **Karla Wasserloos**[b], **Mackenzie Mosher**[b], **Michael W. Epperly**[c], **Joel S. Greenberger**[c], **Bruce R. Pitt**[b], and **Valerian E. Kagan**[a,b,1]

[a]Center for Free Radical and Antioxidant Health, University of Pittsburgh, Pittsburgh, Pennsylvania 15219

[b]Department of Environmental and Occupational Health, Graduate School of Public Health, University of Pittsburgh, Pittsburgh, Pennsylvania 15219

[c]Department of Radiation Oncology, School of Medicine, University of Pittsburgh, Pittsburgh, Pennsylvania 15219

Abstract

Oxidative damage plays a significant role in the pathogenesis of γ-radiation-induced lung injury. Endothelium is a preferred target for early radiation-induced damage and apoptosis. Given the newly discovered role of oxidized phospholipids in apoptotic signaling, we performed oxidative lipidomics analysis of phospholipids in irradiated mouse lungs and cultured mouse lung endothelial cells. C57BL/6NHsd female mice were subjected to total-body irradiation (10 Gy, 15 Gy) and euthanized 24 h thereafter. Mouse lung endothelial cells were analyzed 48 h after γ irradiation (15 Gy). We found that radiation-induced apoptosis *in vivo* and *in vitro* was accompanied by non-random oxidation of phospholipids. Cardiolipin and phosphatidylserine were the major oxidized phospholipids, while more abundant phospholipids (phosphatidylcholine, phosphatidylethanolamine) remained non-oxidized. Electrospray ionization mass spectrometry analysis revealed the formation of cardiolipin and phosphatidylserine oxygenated molecular species in the irradiated lung and cells. Analysis of fatty acids after hydrolysis of cardiolipin and phosphatidylserine by phospholipase A_2 revealed the presence of mono-hydroperoxy and/or mono-hydroxy/mono-epoxy, mono-hydroperoxy/mono-oxo molecular species of linoleic acid. We speculate that cyt c-driven oxidations of cardiolipin and phosphatidylserine associated with the execution of apoptosis in pulmonary endothelial cells are important contributors to endothelium dysfunction in γ-radiation-induced lung injury.

[1]Address for correspondence: Center for Free Radical and Antioxidant Health, Department of Environmental and Occupational Health, University of Pittsburgh, Bridgeside Point, 100 Technology Drive, Suite 350, Pittsburgh, PA; yyt1@pitt.edu; kagan@pitt.edu.

SUPPLEMENTARY INFORMATION

Supplementary Fig. 1. MS/MS fragmentation of CL species with m/z1529.9 from irradiated lung. Supplementary Fig. 2. MS/MS fragmentation of CL species with m/z1497.9 from control lung. Supplementary Fig. 3. Identification of oxygenated fatty acids in CL obtained from the lung of mice after TBI. Supplementary Fig. 4. Identification of oxidized PS molecular species from the lung of mice after TBI. http://dx.doi.org/10.1667/RR2297.1.S1

INTRODUCTION

Lipids are one of the major targets for radicals generated by radiation exposure (1-3). At high doses, lipid peroxidation has been observed in irradiated model systems, including cells *in vitro* (3-6). In addition, increased levels of the secondary lipid peroxidation products thiobarbituric acid-reactive substances (TBARS) and 4-hydroxynonenal were reported in animal models (1, 6, 7) and in patients after total-body irradiation (TBI) (8). While peroxidation of phospholipids yields a large variety of primary and secondary oxygenated and decomposition products (9, 10), the process proceeds via the initial formation of phospholipid hydroperoxides, the most representative primary molecular peroxidation products (11). Nonetheless, the participation and signaling roles of oxidatively modified phospholipids in lung injury induced by TBI including radiation-induced pulmonary endothelial cell apoptosis have not yet been established.

Oxygenated fatty acids are well-known signaling molecules that participate in the regulation and coordination of cellular and body metabolism (12, 13). Their role in cell proliferation, apoptosis, angiogenesis, inflammation and immune surveillance has been well documented (14-16). The involvement of an oxygenated product of polyunsaturated docosahexaenoic acid, resolvin E1, in the pathogenesis of inflammatory lung injury has also been suggested (17, 18). Furthermore, oxidized phospholipids have been demonstrated to act as signals in monocyte activation, programmed cell death and clearance of apoptotic cells by macrophages (19-22).

Apoptosis of pulmonary endothelial cells is an important feature of radiation-induced lung injury and is a critical event underlying early radiation-induced responses (23). Within hours after irradiation, endothelial cells undergo changes related to apoptotic cell death pathways (24-26). Radiation-induced apoptosis of endothelial cells appears to be the major cause of the high radiation sensitivity of the vascular system (25-27). Irradiated endothelial cells also exhibit alterations in the synthesis and secretion of a variety of biomolecules such as growth factors, chemo-attractants and specific injury markers. It is believed that these processes in irradiated endothelium depend to a large extent on radiation-induced activation of acid sphingomyelinases and the generation of ceramide that triggers the mitochondrial apoptotic pathway (28). Late vascular effects occur within months after irradiation and include capillary collapse, thickening of basement membrane, scarring of the surrounding tissue as well as telangiectasias, and a loss of clonogenic capacity (23, 26, 27, 29).

Two anionic phospholipids, a mitochondria-specific cardiolipin (CL) and extramitochondrial phosphatidylserine (PS), have been identified as oxidation substrates of cytochrome c (cyt c)-catalyzed reactions *in vitro* and *in vivo* during execution of apoptosis induced by different stimuli, including γ radiation (30-33). In particular, accumulation of CL-hydroperoxides (CL-OOH) has been associated with a release of proapoptotic factors from mitochondria into the cytosol (34), while PS hydroperoxides (PS-OOH) have been reported to be essential for PS externalization on the surface of plasma membrane (22, 35). Both extrinsic (cell death receptor-mediated) and intrinsic (mitochondria-mediated) apoptosis are recognized as prominent parts of radiation-induced cell death pathways (28, 36-39).

In the present study, we employed oxidative lipidomics to explore the formation and possible involvement of different molecular species of phospholipids in pulmonary endothelial apoptosis induced by γ radiation. We documented selective oxidation of two anionic lipids, CL and PS, in the lungs of mice after TBI. To determine whether these events were intrinsic to a sensitive compartment of lung, similar experiments were repeated in irradiated murine lung endothelial cells (MLECs). Based on previous findings and the results of this work, we speculate that oxidation of CL and PS, possibly catalyzed by cyt c,

is associated with the signaling roles of these oxygenated phospholipid species in the execution of apoptosis and clearance of pulmonary endothelial cells, thus contributing to radiation-induced acute lung injury.

MATERIALS AND METHODS

Total-Body Irradiation (TBI)

Groups of C57BL/6NHsd female mice were irradiated with 0, 10 or 15 Gy TBI using a J. L. Shepherd Mark 1 Model 68 cesium irradiator at a dose rate of 80 cGy/min. Mice were euthanized 24 h later by CO_2 inhalation. Lungs were perfused, removed, washed in PBS and frozen in liquid nitrogen. All procedures were approved and performed according to the protocols established by the Institutional Animal Care and Use Committee of the University of Pittsburgh.

Isolation of Murine Lung Endothelial Cells (MLECs)

Mice were euthanized by CO_2 inhalation and the chest was opened. Lungs were flushed with HBSS containing 10 U/ml heparin and excised lungs were finely minced and digested in type I collagenase. The mixture was filtered, centrifuged, resuspended and incubated with magnetic beads coated with antibody (rat anti-mouse) to PECAM-1 (BD Pharmingen). Magnetic beads were removed gently by a series of rinses (trypsin/EDTA) and the cells were isolated for subculture. At approximately passage 2, cells were incubated with fluorescently labeled diacetylated LDL (diI-LDL) and sorted to homogeneity by FACS. The enriched PECAM and diI-LDL population was subcultured on a collagen/gelatin matrix in 2% O_2, 5% CO_2, 93% N_2 in a Coy Hypoxic Glove Box/Chamber in Opti-MEM (Gibco), 10% FBS, 2 m*M* glutamine, 0.2% retinal derived growth factor (Vec Technologies), 10 U/ml heparin, 0.1 m*M* non-essential amino acid supplement (Gibco), and 55 μ*M* β-mercaptoethanol.

Exposure of MLECs to γ Radiation

Cultured MLECs were plated in full MLEC medium and grown in a hypoxic chamber (2% O_2, 5% CO_2, balance N_2) for 2 days before irradiation. Before irradiation the medium was replaced with OptiMEM + 10% FBS. We used a XRad 160 irradiator (Precision X-Ray, Inc) calibrated with a PTW Unidos E dosimeter TN 30010 Farmer Chamber that allows for irradiation of cells in the same flasks in which they were grown. Irradiation with 15 Gy (160 kVp, 2 mm aluminum, 4.4 Gy/min) was completed within 200 s. During irradiation, flasks with cells (in 2% oxygen) were tightly sealed with parafilm. Thus cells were irradiated in an atmosphere of 2% oxygen. Forty-eight hours after irradiation, cells were trypsinized, washed with PBS, counted and used for assessment of caspase 3/7 activity and lipid analysis.

Caspase 3/7 activity in lung homogenates as well as in MLECs was measured using a luminescence Caspase-Glo™ assay kit obtained from Promega (Madison, WI). Luminescence was determined at time zero and after 1 h incubation at 25°C using an ML1000 luminescence plate reader (Dynatech). Caspase 3 activity was expressed as the luminescence produced within 1 h incubation per μg of protein.

Lipid Extraction and 2D-HPTLC Analysis

Total lipids were extracted from lung homogenates and MLEC using the procedure of Folch *et al*. (40) with some modifications that allowed highly reproducible quantitative analysis of all lipid fractions, including anionic phospholipids and oxidatively modified phospholipids (41-43). The modified Folch procedure included a 20-fold excess of solvent vs tissue and cells (v/v) and a longer extraction time (overnight at 4°C). After this, an additional re-extraction of phospholipids from the methanol/aqueous phase was performed by adding

chloroform (in the amount equal to that of the lower chloroform-enriched phase). We have validated this extraction procedure using different tissue samples and results in the literature (32, 33, 44-48). Almost 99% of phospholipids were recovered by this procedure. Addition of an antioxidant such as butylated hydroxyltoluene (BHT) to samples during lipid extraction interferes with the phospholipid hydroperoxide assay. Therefore, instead of addition of an antioxidant, the procedure of phospholipid extraction and analysis was performed under N_2. The lipidomics analysis was conducted immediately after the extraction. The sufficiency of these preventive strategies was confirmed by our results demonstrating non-random peroxidaton of CL and PS, whereas abundant and polyunsaturated phospholipids such as phosphatidylethanolamine (PE) and phosphatidylcholine (PC) remained non-oxidized and readily detectable in the lung or in lung endothelial cells. Lipid extracts were separated and analyzed by 2D-HPTLC (49). To prevent oxidative modification of phospholipids during separation, plates were treated with methanol containing 1 m*M* EDTA and 100 μ*M* DTPA prior to application and separation of phospholipids by 2D-HPTLC. To minimize possible auto-oxidation of lipids during migration of lipids on the sorbent, we used chelators of metals, particularly of adventitious iron and copper, known to catalyze peroxidation of lipids. Because EDTA and DTPA are the two most widely used metal chelating agents, we pretreated HPTLC plates with methanol containing 1 m*M* EDTA and 100 μ*M* DTPA to remove any metals present on the silica surface of HPTLC plates. EDTA binds divalent metals such as Ca^{2+} and Mg^{2+} with stability constants (log Ks) of 10.7 and 13.6, respectively. EDTA also effectively binds transition metals with stability constants (log Ks) of 25.1 and 18.8 for Fe^{3+} and Cu^{2+}, respectively. However, these bound metals remain redox-active in the presence of reductants (50, 51). DTPA is a more effective chelator of Fe^{3+} and $Cu^{2+}$with log Ks of 27.5 and 21.2, respectively (52). DTPA complexes of transition metals do not undergo redox cycling. Therefore, we used a combination of EDTA and DTPA to provide the most efficient binding and inhibition of possible redox activity of transition metals on silica plates (51). Total lipids (60 nmol) were applied onto plates under flow of N_2 and the plates were first developed with a solvent system consisting of chloroform:methanol:28% ammonium hydroxide (65:25:5 v/v). After the plates were dried with a forced N_2 blower to remove the solvent, they were developed in the second dimension with a solvent system consisting of chloroform:acetone:methanol:glacial acetic acid:water (50:20:10:10:5 v/v). The phospholipids were visualized by exposure to iodine vapors and identified by comparison with authentic phospholipid standards. For electrospray ionization mass spectrometry (ESI-MS) and analysis of phospholipid hydroperoxides (PL-OOH) by fluorescence HPLC using Amplex Red, the phospholipid spots on the silica plates were visualized by spraying the plates with deionized water. Then the spots were scraped from the silica plates and phospholipids were extracted in chloroform:methanol:water (10:5:1 v/v). Lipid phosphorus was determined by a micro-method (53).

Quantification of Lipid Hydroperoxides

PL-OOH were determined by fluorescence HPLC of resorufin formed in peroxidase-catalyzed reduction of specific PL-OOH with Amplex Red after hydrolysis by porcine pancreatic phospholipase A_2 (1 U/μl) in 25 m*M* phosphate buffer containing 1.0 m*M* Ca, 0.5 m*M* EGTA and 0.5 m*M* SDS (pH 8.0 at room temperature for 30 min). For the peroxidase reaction, 50 μ*M* Amplex Red and microperoxidase-11 (1.0 μg/μl) were added to the hydrolyzed lipids, and the samples were incubated at 4°C for 40 min. The reaction was started by addition of microperoxidase-11 and terminated by a stop reagent (100 μl of a solution of 10 m*M* HCl and 4 m*M* butylated hydroxytoluene in ethanol). The samples were centrifuged at 10,000*g* for 5 min and the supernatant was used for HPLC analysis. Aliquots (5 μl) were injected into a C-18 reverse-phase column (Eclipse XDB-C18, 5 μm, 150 × 4.6 mm) and eluted using a mobile phase composed of 25 m*M* KH_2PO_4 (pH 7.0):methanol (60:40 v/v) at a flow rate of 1 ml/min. The resorufin fluorescence was measured at 590 nm

after excitation at 560 nm. Shimadzu LC-100AT *vp* HPLC system equipped with a fluorescence detector (model RF-10Axl) and an autosampler (model SIL-10AD *vp*) was used (46).

ESI-MS

ESI-MS analysis was performed by direct infusion into linear ion-trap mass spectrometer LXQ™ with the Xcalibur operating system (Thermo Fisher Scientific, San Jose, CA) as described previously (46). Samples collected after 2D-HPTLC separation were evaporated under N_2, resuspended in chloroform:methanol 1:1 v/v (20 pmol/μl), and used for acquisition of negative-ion or positive-ion ESI mass spectra at a flow rate of 5 μl/min. The ESI probe was operated at a voltage differential of 3.5–5.0 kV in the negative- or positive-ion mode. Capillary temperature was maintained at 70 or 150°C. Using full-range zoom (200–2000 *m/z*) in positive- and negative-ion mode, the profile spectra were acquired. Tandem mass spectrometry (MS/MS analysis) of individual phospholipid species was employed to determine the fatty acid composition. The MS/MS spectra were acquired using an isolation width of 1.0 *m/z*. Singly charged ions were used for structural identification of CL as described by Hsu and coauthors (54). The scan time setting of ion trap for full MS (range 1400–1600 *m/z*) was 50 microscans with a maximum injection time of 1000 ms. MS^n analysis was performed using an isolation width of 1 *m/z* and 5 microscans with a maximum injection time of 1000 ms. Two ion activation techniques were used for MS analysis: collision-induced dissociation (CID, Q = 0.25, low mass cutoff at 28% of the precursor *m/z*) and pulsed-Q dissociation technique (PQD, with Q = 0.7 and no low mass cutoff for analysis of low-molecular-weight fragment ions). Based on the MS fragmentation data, the chemical structures of lipid molecular species were drawn using ChemDraw and confirmed by comparing with the fragmentation patterns presented in the Lipid Map Data Base (www.lipidmaps.org).

LC/ESI-MS of Phospholipids

To quantitatively assess different molecular species of CL and PS, LC/ESI-MS was performed using a Dionex Ultimate™ 3000 HPLC coupled online to ESI and a linear ion-trap mass spectrometer (LXQ Thermo-Fisher). The lipids were separated on a normal-phase column (Luna 3 μm Silica 100A, 150 × 2 mm, Phenomenex, Torrance, CA) with a flow rate of 0.2 ml/min using gradient solvents containing 5 m*M* CH_3COONH_4 [A, n-hexane:2-propanol:water, 43:57:1 (v/v/v); B, n-hexane:2-propanol:water, 43:57:10 (v/v/v)]. Analysis of phospholipid oxidized molecular species was performed as described previously (46). To account for isotopic interferences, we performed isotopic corrections by entering the chemical composition of each species into the Qual browser of Xcalibur (operating system) and using the simulation of the isotopic distribution to make adjustments for the major peaks. To minimize isotopic interferences between isolated masses M + 2, the MS/MS spectra were acquired using an isolation width of 1.0 *m/z*.

LC/ESI-MS of Oxygenated Fatty Acids

Oxygenated fatty acids were analyzed by LC/ESI-MS after hydrolysis of major classes of phospholipids with porcine pancreatic phospholipase A_2 (1 U/μl) in 25 m*M* phosphate buffer containing 1.0 m*M* Ca, 0.5 m*M* EGTA and 0.5 m*M* SDS (pH 8.0 at room temperature for 30 min). Aliquots of extracted lipids (5 μl) were injected into a C-18 reverse-phase column (Luna, 3 μm, 150 × 2 mm) and eluted using gradient solvents (A and B) containing 5 m*M* CH_3COONH_4 at a flow rate of 0.2 ml/min. Solvent A was 25:30:50:0.1 tetrahydrofuran:methanol:water:CH_3COOH (v/v/v/v). Solvent B was 90:10 methanol:water (v/v). The column was eluted during the first 3 min isocratically at 50% B, from 3 to 23 min with a linear gradient from 50% solvent B to 98% solvent B, then 23–40 min isocratically using 98% solvent B, 40–42 min with a linear gradient from 98% solvent B to 50% solvent

B, 42–28 min isocratically using 50% solvent B for equilibration of the column. The hydroperoxy-fatty acids 13S-hydroperoxy-9Z,11E-octadecadienoic acid, 9-hydroxy-10E, 12Z-octadecadienoic acid, and 15S-hydroperoxy-5Z,8Z,11Z13E-eicosatetraenoic acid from Cayman chemicals (Ann Arbor, MI) were used as standards.

Statistics

The results are presented as means ± SD from at least three experiments. Statistical analyses were performed with either a paired/unpaired Student's *t* test or one-way ANOVA. Statistical significance was set at $P < 0.05$

RESULTS

Effect of TBI on Phospholipid Composition of Mouse Lung

The effects of radiation (10 Gy and 15 Gy) on the composition of major phospholipids in mouse lung were assessed by 2D-HPTLC (Fig. 1A inset). To quantify phospholipids, the silica spots were scraped off the plates and lipid phosphorus was determined. No significant changes in the composition of phospholipids were detected in mouse lung after TBI (Fig. 1A).

Effect of TBI on the Accumulation of Hydroperoxy Phospholipids in the Mouse Lung

The amounts of PL-OOH in major phospholipid fractions were detected using the HPLC Amplex Red protocol. Two phospholipids, CL and PS, underwent oxidation in the lung after TBI (Fig. 1B). CL-OOH and PS-OOH contents increased after exposure to 10 and 15 Gy compared to the control lung. Radiation-induced increments of CL-OOH and PS-OOH constituted 4.9 and 15.5 pmol/nmol CL and 8.0 and 6.9 pmol/nmol PS at 10 and 15 Gy, respectively. No significant oxidation in the other major phospholipid classes such as PC, PE and phosphatidylinositol (PI) was detected in lungs of irradiated animals.

ESI-MS Analysis of CL and PS Molecular Species of Lung Phospholipids

Molecular species of CL and PS were characterized by ESI-MS using the negative mode. Direct infusion experiments as well as LC/ESI-MS were employed in MS and MS/MS analyses for identification of the molecular species containing polyunsaturated fatty acid residues that are highly susceptible to oxidation. Typical full ESI-MS spectra of lung phospholipids are presented in Fig. 2A. All phospholipids contained highly unsaturated fatty acid residues with two-six double bonds. The results of the identification of phospholipids are presented as a lipid profile map in Fig. 2B.

ESI-MS Analysis of CL Molecular Species of Lung Phospholipids

Given that quantitative assessment of PL-OOH in irradiated lung showed that CL and PS underwent oxidative modification after TBI, we focused on identification of their oxidation products using both direct infusion ESI-MS and LC/ESI-MS. LC/MS analysis of CL molecular species from control lung revealed major CL molecular clusters at *m/z* 1449.9 and 1473.9 (Figs. 2A and 3A, a). Molecular clusters at *m/z* 1421.9, 1497.9 and 1521.9 were also detectable in the full MS spectrum but at relatively lower abundances. Fragmentation analysis showed that CL was enriched with molecular species containing linoleic acid ($C_{18:2}$). Arachidonic ($C_{20:4}$), docosapentaenoic ($C_{22:5}$) and docosahexaenoic ($C_{22:6}$) acyls were also present in CL molecules but at lower abundances (Fig. 2B).

ESI-MS Analysis of Oxidized CL Molecular Species of Lung Phospholipids

Quantitative assessments of radiation-induced changes in CL revealed a significant reduction of less abundant but more unsaturated species of CL with *m/z* 1495.9 and 1497.9

(Fig. 3B, a). The amount of these molecular species was decreased 2.1- and 1.7-fold and 2.0- and 1.4-fold, respectively, after TBI with doses of 10 Gy and 15 Gy compared to the control mice (Fig. 3B, a). The amounts of molecular species with *m/z* 1521.9, 1525.9 were also reduced 1.3- and 3.6-fold and 1.3- and 1.2-fold, respectively, after TBI with doses of 10 Gy and 15 Gy compared to control mice (Fig. 3B, b). No significant changes were found in clusters of less polyunsaturated CL molecules with *m/z* 1447.9–1451.8 and 1471.9–1479.9.

The loss of "oxidizable" CLs was accompanied by the appearance of their oxygenated species, as illustrated by a typical fragmentation pattern of the CL molecular ion with *m/z* 1529.9 (Supplementary Fig. 1). The MS/MS analysis showed that this oxidized molecular species originated from the molecular species with *m/z* 1497.9 (Supplementary Fig. 2) after addition of two oxygen atoms. Molecular ion with *m/z* 1497.9 was represented by three highly unsaturated molecular species: $C_{18:2}/C_{20:4}/C_{20:4}/C_{18:1}$, $C_{18:2}/C_{18:2}/C_{18:2}/C_{22:5}$ and $C_{18:1}/C_{18:2}/C_{18:2}/C_{22:6}$ (Supplementary Fig. 2). The molecular ion with *m/z* 1529.9 was identified as peroxidized CL molecular species containing mono-hydroperoxy-$C_{18:2}$ ($C_{18:1}/C_{18:2\text{-}OOH}/C_{18:2}/C_{22:6}$) and two mono-hydroxy-$C_{20:4}$ ($C_{18:2}/C_{20:4\text{-}OH}/C_{20:4\text{-}OH}/C_{18:1}$) (Supplementary Fig. 1). Oxidized molecular species of CL with *m/z* 1527.9, which originated from the molecular ion with *m/z* 1495.9 after the addition of two oxygens, were also detected (data not shown).

To further quantitatively assess and structurally characterize oxygenated fatty acids in the *sn*-2 position of oxidized CL species, lipids from control and irradiated lungs were separated by 2D-HPTLC; CL fractions were collected and treated with phospholipase A_2. The fatty acids obtained by hydrolysis were analyzed by LC/ESI-MS. Peaks with retention times of 9.44 min (*m/z* 311) and 12.28 min (*m/z* 325) were detected on LC/MS chromatograms of lipids from lungs of irradiated mice (Fig. 4A a, b). MS/MS analysis of the peak with *m/z* 311 revealed the presence of two overlapping isomers of mono-hydroperoxy-$C_{18:2}$ and two overlapping isomers of mono-hydroxy/mono-epoxy-$C_{18:2}$ that were identified as 13-hydroperoxy-$C_{18:2}$, 9-hydroperoxy-$C_{18:2}$ and 13-hydroxy,9-10-epoxy-$C_{18:2}$, 9-hydroxy, 12-13-epoxy-$C_{18:2}$, respectively (Supplementary Fig. 3). Two other oxidation products of $C_{18:2}$ (13-oxo-,8-hydroxy-$C_{18:2}$; 9-oxo,14-hydroxy-$C_{18:2}$) were detected during fragmentation of molecular ions with *m/z* 325 (Supplementary Fig. 3). Quantitative assessment of oxygenated $C_{18:2}$ revealed a significant and dose-dependent increase of mono-hydroperoxy-, mono-hydroxy/mono-epoxy- and mono-hydroperoxy/mono-oxo-molecular species of $C_{18:2}$ in irradiated lungs (Fig. 4A, B). Molecular ions with *m/z* 309 (oxo-$C_{18:2}$) and *m/z* 319 (hydroxy-$C_{20:4}$) were also detected on LC chromatograms but at a lower abundance (data not shown). The levels of oxygenation of $C_{20:4}$ in the lung CL after TBI were significantly lower than those of $C_{18:2}$ and at 15 Gy did not exceed 1.4 pmol/nmol CL. Thus not only were less abundant molecular species of CL containing $C_{18:2}$, $C_{20:4}$, $C_{22:5}$ and $C_{22:6}$ fatty acids subject to radiation-induced oxidation but relatively less polyunsaturated $C_{18:2}$ fatty acid residues were also preferable oxidation substrates in the mouse lung. This demonstrates the specific, non-random nature of radiation-induced oxidation of CL in the lung.

ESI-MS Analysis of PS and its Oxidized Molecular Species in the Mouse Lung

In the mouse lung, PS was represented by three major molecular clusters with *m/z* 788.5, 810.5 and 834.5 containing $C_{18:0}$, $C_{18:1}$, $C_{20:4}$, $C_{22:5}$ and $C_{22:6}$ (Figs. 2A and 5A). A comparative LC/ESI-MS analysis of PS isolated from normal and irradiated lungs demonstrated a significant decrease in the intensity of less abundant molecular ions with *m/z* 786.5 corresponding to PS-$C_{18:0}/C_{18:2}$ (Fig. 5B). MS/MS analysis of this molecular species revealed the presence of daughter ions at *m/z* 283 and *m/z* 279 corresponding to $C_{18:0}$ and $C_{18:2}$ along with other ions typical for PS fragmentation (Supplementary Fig. 4A). We found that the amounts of PS-$C_{18:0}/C_{18:2}$ were reduced in the lungs of mice exposed to 10 Gy and

15 Gy compared to control lung (Fig. 5C). It is possible that these molecular species were oxidized in the mouse lung after TBI. Detailed analysis of oxidized PS molecular species with *m/z* 818.5 and 832.5 demonstrated that they originated from a molecular species of PS-$C_{18:0}$/$C_{18:2}$ (*m/z* 786.5) after the addition of 2 and 3 oxygens and corresponded to $C_{18:0}$/$C_{18:2+2O}$ and $C_{18:0}$/$C_{18:2+3O}$, respectively (Supplementary Fig. 4B and C).

Similar to CL, molecular ions with *m/z* 311 (Fig. 6A, a) and 325 (Fig. 6B, a) were detectable on base-peak LC/MS chromatograms obtained after hydrolysis of PS by phospholipase A_2. MS/MS fragmentation showed that molecular ions with *m/z* 311 and 325 corresponded to 13-hydroperoxy-$C_{18:2}$, 9-hydroperoxy-$C_{18:2}$, 13-hydroxy, 9-10-epoxy-$C_{18:2}$, 9-hydroxy, 12-13-epoxy-$C_{18:2}$, and 13- oxo-,8-hydroxy-$C_{18:2}$; 9-oxo,14-hydroxy-$C_{18:2}$, respectively (data not shown). Radiation caused a significant dose-dependent accumulation of mono-hydroperoxy-, mono-hydroxy/mono-epoxy- and mono-hydroperoxy/mono-oxo- molecular species of $C_{18:2}$ (Fig. 6A, b and B, b) in the lung. Small amounts of these oxygenated $C_{18:2}$ derivatives were detected in the control lung. No other oxygenated fatty acids were detected.

Radiation-Induced Apoptosis in Mouse Lung

Our previous studies established an association of selective peroxidation of CL and PS with the initiation and progression of apoptosis and clearance of apoptotic cells by professional phagocytes (22, 34). Therefore, we determined whether selective oxidation of CL and PS was accompanied by radiation-induced apoptosis. We found that caspase 3/7 activity was significantly increased in the lungs of mice after TBI compared to control nonirradiated mice (Fig. 7). A 2.5- and 4.5-fold increase in caspase 3/7 activity was detected after the exposure to 10 Gy and 15 Gy, respectively (Fig. 7).

ESI-MS Analysis of Phospholipid Molecular Species in MLECs Exposed to γ Radiation

We performed oxidative lipidomics studies of control MLECs and MLECs 48 h after γ irradiation since pulmonary endothelium is known to be a critical target of radiation-induced lung injury (23). Similar to the results obtained for whole lung, irradiation of MLECs resulted in oxidation of only two phospholipids: CL and PS. Decreased intensity of CL molecular ions with *m/z* 1423.9, *m/z* 1427.9, *m/z* 1447.9 and *m/z* 1473.9 corresponding to molecular species $C_{16:1}$/$C_{18:2}$/$C_{18:2}$/$C_{18:1}$, $C_{16:0}$/$C_{18:2}$/$C_{18:1}$/$C_{18:1}$, $C_{18:2}$/$C_{18:2}$/$C_{18:2}$/$C_{18:2}$ and $C_{18:1}$/$C_{18:2}$/$C_{18:2}$/$C_{20:4}$ was detected in LC/MS spectrum of CL from irradiated cells (Fig. 8A, a, b). In addition, a significant decrease of PS-$C_{18:0}$/$C_{18:2}$ molecular species was detected in irradiated cells (Fig. 8B, a and b). A 2-fold activation of caspase 3/7 occurred in MLECs 48 h after γ irradiation (Fig. 8C).

DISCUSSION

Pulmonary endothelium is likely to be a preferred target for early radiation-induced damage and cell death, which occur to a large extent via apoptotic pathways (23, 36, 55). The acute vascular changes within 24 h are dominated by the radiation-induced apoptosis of endothelial cells (23). Radiolysis of water and generation of reactive radicals initiate oxidative modification of essential intracellular molecules, culminating in DNA damage and triggering apoptosis through p53-dependent pathways (23, 56). Radiation-activated p53 can trigger intrinsic (mitochondria-dependent) apoptosis through regulation of BAX and Bcl2 proteins (57-59). Furthermore, activated p53 can upregulate the extrinsic (death receptor-dependent) apoptotic mechanisms (56). This may include radiation-induced activation of sphingomyelinase and generation of ceramide in endothelial cells (55). The latter will interact with TNF receptor to trigger apoptosis (23, 55). In line with the activation of apoptotic mechanisms, we found marked dose-dependent increases in caspase 3 and 7

activity in the lungs of mice after TBI. A 2-fold activation of caspases 3 and 7 also occurred in MLECs 48 h after γ irradiation.

Oxidative damage has been suggested to play a significant role in pathogenesis of radiation-induced lung injury. Lipids were determined to be one of the major targets for radicals generated by radiation in cells *in vitro* (3-6), in animal models (1, 7) and in patients after TBI (8). However, the participation and signaling roles of oxidatively modified phospholipids in pulmonary endothelial apoptosis after radiation-induced injury have not been established. The 24 h postirradiation exposure was chosen since this is the time when the lung cells, particularly endothelial cells, are undergoing apoptosis. We found significantly elevated levels of caspase 3/7 in the lung 24 h after irradiation (23). Thus we speculated that selective peroxidation of CL and PS might be associated with the involvement and signaling roles of these phospholipids in apoptosis. Our previous studies demonstrated essential roles of oxidatively modified CL and PS in the apoptotic mitochondrial membrane permeability transition and PS externalization, respectively. The selectivity of phospholipid peroxidation may be a function of time and may depend, for example, on the involvement of activated inflammatory cells in the process of injury.

We used MLECs as a surrogate for this sensitive compartment of the lung because reliance on biochemical analyses of bulk lung homogenates obscures (Figs. 1-7) the contribution of the pulmonary endothelium and *in situ* approaches such as MS imaging of oxidized lipids have not been applied to this site. Phenotypic drift in culture of primary pulmonary endothelial cells is a well-known phenomenon (60, 61) and presumably accounts for potential differences in sensitivity *in vitro* from predictions *in vivo*. In our case, such confounding elements may have accounted for differences in timing (48 h in MLECs and 24 h in whole lung). Nonetheless, short of extraordinary approaches such as intravital microscopy (62) or whole organ reconstitution on a chip (63), our conventional approach of using MLECs as a surrogate led us to conclude that radiation-induced apoptosis and its association with selective oxidation of CL and PS was an intrinsic property of pulmonary endothelium. In this sense, these radiation-induced changes were independent of the contribution of residential (e.g. smooth muscle, fibroblasts) or migratory (neutrophils, macrophages) cells and were apparent without attendant physiological contributions of the intact lung (neuronal, hormonal, mechanical). It remains to be determined whether other cellular targets of radiation in the lung undergo similar changes.

Recently, we demonstrated that CL and PS oxidations are catalyzed by cyt c that acts as a CL- and PS-specific peroxidase in mitochondria early in apoptosis and later in the inner leaflet of plasma membrane, respectively. CL oxidation products (CL-OOH) are required for the release of pro-apoptotic factors into the cytosol, including cyt c (34). In addition, PS oxidation and formation of PS-OOH is essential for PS externalization and uptake of apoptotic cells by phagocytes (22, 35). Further, γ radiation-induced CL oxidation and apoptosis in HeLa cells were proportional to the content of cyt c manipulated by RNAi (31). In model systems, oxidation of CL and PS driven by cyt c in the presence of H_2O_2 yields CL and PS oxidation products similar to those found in small intestine of mice after TBI (33). Thus it is tempting to speculate that cyt c is involved in oxidation of CL and PS in the lung and pulmonary endothelium induced by γ radiation.

While the mechanisms of selectivity toward CL and PS are likely associated with the catalytic role of cyt c (34), the specificity toward individual molecular species of CL and PS remains to be elucidated. Here, we demonstrate that radiation-induced apoptosis is accompanied by CL and PS oxidation both *in vivo* (whole lung) and *in vitro* (MLECs). Quantitative analysis and structural characterization of oxidizable CL molecular species showed that less abundant molecular species of CL underwent robust oxidation in the lungs

after TBI. More abundant polyunsaturated phospholipids such as PC and PE remained intact after both 10 Gy and 15 Gy TBI. Molecular species of oxidizable CL ($C_{18:2}/C_{20:4}/C_{20:4}/C_{18:1}$, $C_{18:1}/C_{18:2}/C_{18:2}/C_{22:6}$) were oxygenated after TBI. We identified esterified linoleic acid as the main substrate of irradiation induced CL oxidation in the lung. The oxygenated species of $C_{18:2}$ were identified as 13-hydroperoxy-$C_{18:2}$, 9-hydroperoxy-$C_{18:2}$, 13-hydroxy, 9-10-epoxy-$C_{18:2}$, 9-hydroxy,12-13-epoxy-$C_{18:2}$, 13-oxo-,8-hydroxy-$C_{18:2}$, and 9-oxo,14-hydroxy-$C_{18:2}$. While the formation of hydroperoxy-CLs *in vivo* may stem directly from the oxygenase reaction catalyzed by cyt c, the catalytic mechanisms involved in the production of oxo- and epoxy-derivatives and identification of specific protein participants need further study. The formation of oxo- and epoxy-derivatives of linoleic acid by cyt c in the presence of CL has been demonstrated in a model system (64) as well as in isolated submitochondrial particles (65). Moreover, formation of oxo-linoleic acid can be catalyzed by hydroxyoctadecadienoic acid dehydrogenase. Partial purification and characterization of 13-hydroxyoctadecadienoic dehydrogenase from rat tissues has been reported (66).

We also found that less polyunsaturated and less abundant molecular species of PS, $C_{18:0}/C_{18:2}$ underwent robust oxidation in the lung of irradiated mice. Previously, we demonstrated that cyt c released from mitochondria into the cytosol can bind PS and cause its peroxidation via the same peroxidase mechanisms to yield hydroxy- and hydroperoxy-species of PS. The signaling role of oxidized PS is realized through its participation in facilitating PS externalization and the appearance of PS and its oxidation products on the surface of apoptotic cells (35). Both PS and PS oxidation products are recognition signals for several receptors and subsequent clearance by macrophages (19, 22).

Further support for a role for cyt c peroxidase-mediated selective oxidation of CL and PS in radiation-induced apoptosis of pulmonary endothelium is provided by comparison with two other models of oxidant-mediated apoptosis in pulmonary endothelium. In particular, we recently demonstrated that hyperoxia (48) and LPS (47) caused apoptosis in cultured pulmonary artery endothelial cells that was also associated with selective oxidation of CL and PS. In hyperoxia, we noted that a mitochondrial-targeted antioxidant disrupted such selective oxidation and inhibited apoptosis (48). It should be noted that apoptosis-associated selective peroxidation of CL and PS is not unique to the mechanism of radiation injury. Recently, using a hyperoxia model of acute lung injury, we demonstrated that endothelial apoptosis was paralleled by accumulation of CL and PS oxidation products *in vivo* (48).

The most prevalent phospholipids in surfactant are saturated phospholipids such as phosphatidylcholine (PC) (>85%), particularly dipalmitoyl-PC, that do not undergo peroxidation. In line with this, we did not find any radiation-induced oxidation of PC. Phosphatidylglycerol (PG) is accountable for about 11% of the surfactant lipids (67, 68). The surfactant PG is also represented by poorly oxidizable saturated and mono-unsaturated molecular species. Finally, small amounts of phosphatidylinositol (PI), less than 4%, have been found in the surfactant that contains polyunsaturated potentially oxidizable species (68). No significant accumulation of PI oxidation products in lung of mice was found after TBI.

At this time we cannot quantitatively estimate the contribution of epithelial cells in the generation of oxygenated species of CL and PS induced by radiation. Taking into account that endothelial cells respond to radiation within first 24 h (23), we suggested that phospholipids of pulmonary endothelial cells are a major target of radiation-induced oxidation. Indeed, we found that the profile of oxygenated phospholipids induced by radiation in the whole lung was similar to that in irradiated lung endothelial cells. Thus our data are compatible with the essential role of pulmonary endothelium as an important

contributor to CL and PS peroxidation in acute lung injury during the first 24–48 h after irradiation.

Overall our results imply that a non-random, likely enzymatic mechanism(s) is involved in catalysis of lipid peroxidation in lungs of mice after TBI. We speculate that the cyt c-driven oxidation of CL and PS is associated with the execution of apoptosis in pulmonary endothelial cells, thus contributing to radiation-induced lung injury. This indicates promising routes for the discovery of novel radioprotectors and radiomitigators.

Supplementary Material

Refer to Web version on PubMed Central for supplementary material.

Acknowledgments

This research was supported by NIH Grants HL70755, HL094488, HL65697, CA119927 and U19 AI068021.

References

1. Kergonou JF, Bernard P, Braquet M, Rocquet G. Effect of whole-body gamma irradiation on lipid peroxidation in rat tissues. Biochimie. 1981; 63:555–559. [PubMed: 7260175]
2. Schwenke K, Coslar S, Muhlensiepen H, Altman KI, Feinendegen LE. Lipid peroxidation in microsomes of murine bone marrow after low-dose gamma-irradiation. Radiat Environ Biophys. 1994; 33:315–323. [PubMed: 7708905]
3. Nakazawa T, Nagatsuka S. Radiation-induced lipid peroxidation and membrane permeability in liposomes. Int J Radiat Biol Relat Stud Phys Chem Med. 1980; 38:537–544. [PubMed: 6969701]
4. Nakajima T, Yukawa O. Radiation-induced translocation of protein kinase C through membrane lipid peroxidation in primary cultured rat hepatocytes. Int J Radiat Biol. 1996; 70:473–480. [PubMed: 8862459]
5. Srinivasan M, Sudheer AR, Pillai KR, Kumar PR, Sudhakaran PR, Menon VP. Lycopene as a natural protector against gamma-radiation induced DNA damage, lipid peroxidation and antioxidant status in primary culture of isolated rat hepatocytes *in vitro*. Biochim Biophys Acta. 2007; 1770:659–665. [PubMed: 17189673]
6. Prasad NR, Menon VP, Vasudev V, Pugalendi KV. Radioprotective effect of sesamol on gamma-radiation induced DNA damage, lipid peroxidation and antioxidants levels in cultured human lymphocytes. Toxicology. 2005; 209:225–235. [PubMed: 15795059]
7. Umegaki K, Aoki S, Esashi T. Whole body X-ray irradiation to mice decreases ascorbic acid concentration in bone marrow: comparison between ascorbic acid and vitamin E. Free Radic Biol Med. 1995; 19:493–497. [PubMed: 7590399]
8. Facorro G, Sarrasague MM, Torti H, Hager A, Avalos JS, Foncuberta M, Kusminsky G. Oxidative study of patients with total body irradiation: effects of amifostine treatment. Bone Marrow Transplant. 2004; 33:793–798. [PubMed: 14990982]
9. Niki E. Lipid peroxidation: physiological levels and dual biological effects. Free Radic Biol Med. 2009; 47:469–484. [PubMed: 19500666]
10. Catala A. Lipid peroxidation of membrane phospholipids generates hydroxy-alkenals and oxidized phospholipids active in physiological and/or pathological conditions. Chem Phys Lipids. 2009; 157:1–11. [PubMed: 18977338]
11. Kagan, VE. Lipid Peroxidation in Biomembranes. CRC Press; Boca Raton, FL: 1988.
12. Shearer GC, Newman JW. Impact of circulating esterified eicosanoids and other oxylipins on endothelial function. Curr Atheroscler Rep. 2009; 11:403–410. [PubMed: 19852880]
13. Macchia L, Hamberg M, Kumlin M, Butterfield JH, Haeggstrom JZ. Arachidonic acid metabolism in the human mast cell line HMC-1: 5-lipoxygenase gene expression and biosynthesis of thromboxane. Biochim Biophys Acta. 1995; 1257:58–74. [PubMed: 7599181]

14. Tang DG, La E, Kern J, Kehrer JP. Fatty acid oxidation and signaling in apoptosis. Biol Chem. 2002; 383:425–442. [PubMed: 12033433]
15. Serhan CN, Haeggstrom JZ, Leslie CC. Lipid mediator networks in cell signaling: update and impact of cytokines. FASEB J. 1996; 10:1147–1158. [PubMed: 8751717]
16. Haworth O, Levy BD. Endogenous lipid mediators in the resolution of airway inflammation. Eur Respir J. 2007; 30:980–992. [PubMed: 17978156]
17. Aoki H, Hisada T, Ishizuka T, Utsugi M, Kawata T, Shimizu Y, Okajima F, Dobashi K, Mori M. Resolvin E1 dampens airway inflammation and hyperresponsiveness in a murine model of asthma. Biochem Biophys Res Commun. 2008; 367:509–515. [PubMed: 18190790]
18. Haworth O, Cernadas M, Yang R, Serhan CN, Levy BD. Resolvin E1 regulates interleukin 23, interferon-gamma and lipoxin A4 to promote the resolution of allergic airway inflammation. Nat Immunol. 2008; 9:873–879. [PubMed: 18568027]
19. Greenberg ME, Sun M, Zhang R, Febbraio M, Silverstein R, Hazen SL. Oxidized phosphatidylserine-CD36 interactions play an essential role in macrophage-dependent phagocytosis of apoptotic cells. J Exp Med. 2006; 203:2613–2625. [PubMed: 17101731]
20. Maskrey BH, Bermudez-Fajardo A, Morgan AH, Stewart-Jones E, Dioszeghy V, Taylor GW, Baker PR, Coles B, Coffey MJ, O'Donnell VB. Activated platelets and monocytes generate four hydroxyphosphatidylethanolamines via lipoxygenase. J Biol Chem. 2007; 282:20151–20163. [PubMed: 17519227]
21. Cole AL, Subbanagounder G, Mukhopadhyay S, Berliner JA, Vora DK. Oxidized phospholipid-induced endothelial cell/monocyte interaction is mediated by a cAMP-dependent R-Ras/PI3-kinase pathway. Arterioscler Thromb Vasc Biol. 2003; 23:1384–1390. [PubMed: 12805072]
22. Kagan VE, Borisenko GG, Serinkan BF, Tyurina YY, Tyurin VA, Jiang J, Liu SX, Shvedova AA, Fabisiak JP, Fadeel B. Appetizing rancidity of apoptotic cells for macrophages: oxidation, externalization, and recognition of phosphatidylserine. Am J Physiol Lung Cell Mol Physiol. 2003; 285:L1–L17. [PubMed: 12788785]
23. Rodemann HP, Blaese MA. Responses of normal cells to ionizing radiation. Semin Radiat Oncol. 2007; 17:81–88. [PubMed: 17395038]
24. Zhao W, Robbins ME. Inflammation and chronic oxidative stress in radiation-induced late normal tissue injury: therapeutic implications. Curr Med Chem. 2009; 16:130–143. [PubMed: 19149566]
25. Paris F, Fuks Z, Kang A, Capodieci P, Juan G, Ehleiter D, Haimovitz-Friedman A, Cordon-Cardo C, Kolesnick R. Endothelial apoptosis as the primary lesion initiating intestinal radiation damage in mice. Science. 2001; 293:293–297. [PubMed: 11452123]
26. Kwock L, Davenport WC, Clark RL, Zarembra J, Lingle B, Chaney EL, Friedman M. The effects of ionizing radiation on the pulmonary vasculature of intact rats and isolated pulmonary endothelium. Radiat Res. 1987; 111:276–291. [PubMed: 3628716]
27. Ward WF, Sharplin J, Franko AJ, Hinz JM. Radiation-induced pulmonary endothelial dysfunction and hydroxyproline accumulation in four strains of mice. Radiat Res. 1989; 120:113–120. [PubMed: 2552496]
28. Kolesnick R, Fuks Z. Radiation and ceramide-induced apoptosis. Oncogene. 2003; 22:5897–5906. [PubMed: 12947396]
29. Brush J, Lipnick SL, Phillips T, Sitko J, McDonald JT, McBride WH. Molecular mechanisms of late normal tissue injury. Semin Radiat Oncol. 2007; 17:121–130. [PubMed: 17395042]
30. Huang Z, Jiang J, Tyurin VA, Zhao Q, Mnuskin A, Ren J, Belikova NA, Feng W, Kurnikov IV, Kagan VE. Cardiolipin deficiency leads to decreased cardiolipin peroxidation and increased resistance of cells to apoptosis. Free Radic Biol Med. 2008; 44:1935–1944. [PubMed: 18375209]
31. Belikova NA, Jiang J, Tyurina YY, Zhao Q, Epperly MW, Greenberger J, Kagan VE. Cardiolipin-specific peroxidase reactions of cytochrome C in mitochondria during irradiation-induced apoptosis. Int J Radiat Oncol Biol Phys. 2007; 69:176–186. [PubMed: 17707271]
32. Tyurina YY, Tyurin VA, Kapralova VI, Amoscato AA, Epperly MW, Greenberger JS, Kagan VE. Mass-spectrometric characterization of phospholipids and their hydroperoxide derivatives *in vivo*: effects of total body irradiation. Methods Mol Biol. 2009; 580:153–183. [PubMed: 19784599]

33. Tyurina YY, Tyurin VA, Epperly MW, Greenberger JS, Kagan VE. Oxidative lipidomics of gamma-irradiation-induced intestinal injury. Free Radic Biol Med. 2008; 44:299–314. [PubMed: 18215738]
34. Kagan VE, Tyurin VA, Jiang J, Tyurina YY, Ritov VB, Amoscato AA, Osipov AN, Belikova NA, Kapralov AA, Borisenko GG. Cytochrome c acts as a cardiolipin oxygenase required for release of proapoptotic factors. Nat Chem Biol. 2005; 1:223–232. [PubMed: 16408039]
35. Tyurina YY, Tyurin VA, Zhao Q, Djukic M, Quinn PJ, Pitt BR, Kagan VE. Oxidation of phosphatidylserine: a mechanism for plasma membrane phospholipid scrambling during apoptosis? Biochem Biophys Res Commun. 2004; 324:1059–1064. [PubMed: 15485662]
36. Reap EA, Roof K, Maynor K, Borrero M, Booker J, Cohen PL. Radiation and stress-induced apoptosis: a role for Fas/Fas ligand interactions. Proc Natl Acad Sci USA. 1997; 94:5750–5755. [PubMed: 9159145]
37. Sheard MA, Vojtesek B, Janakova L, Kovarik J, Zaloudik J. Up-regulation of Fas (CD95) in human p53wild-type cancer cells treated with ionizing radiation. Int J Cancer. 1997; 73:757–762. [PubMed: 9398058]
38. Haimovitz-Friedman A, Kan CC, Ehleiter D, Persaud RS, McLoughlin M, Fuks Z, Kolesnick RN. Ionizing radiation acts on cellular membranes to generate ceramide and initiate apoptosis. J Exp Med. 1994; 180:525–535. [PubMed: 8046331]
39. Ogura A, Oowada S, Kon Y, Hirayama A, Yasui H, Meike S, Kobayashi S, Kuwabara M, Inanami O. Redox regulation in radiation-induced cytochrome c release from mitochondria of human lung carcinoma A549 cells. Cancer Lett. 2009; 277:64–71. [PubMed: 19117669]
40. Folch J, Lees M, Sloane Stanley GH. A simple method for the isolation and purification of total lipides from animal tissues. J Biol Chem. 1957; 226:497–509. [PubMed: 13428781]
41. Delerive P, Furman C, Teissier E, Fruchart J, Duriez P, Staels B. Oxidized phospholipids activate PPARalpha in a phospholipase A2-dependent manner. FEBS Lett. 2000; 471:34–38. [PubMed: 10760508]
42. Watson AD, Leitinger N, Navab M, Faull KF, Horkko S, Witztum JL, Palinski W, Schwenke D, Salomon RG, Berliner JA. Structural identification by mass spectrometry of oxidized phospholipids in minimally oxidized low density lipoprotein that induce monocyte/endothelial interactions and evidence for their presence *in vivo*. J Biol Chem. 1997; 272:13597–13607. [PubMed: 9153208]
43. Van der Meeren, P.; Van der Deelen, J. Phospholipid analysis by HPLC. In: Nollet, LML., editor. Food Analysis by HPLC. CRC Press; Boca Raton, FL: 2000. p. 251-256.
44. Bayir H, Tyurin VA, Tyurina YY, Viner R, Ritov V, Amoscato AA, Zhao Q, Zhang XJ, Janesko-Feldman KL, Kagan VE. Selective early cardiolipin peroxidation after traumatic brain injury: an oxidative lipidomics analysis. Ann Neurol. 2007; 62:154–169. [PubMed: 17685468]
45. Tyurin VA, Tyurina YY, Feng W, Mnuskin A, Jiang J, Tang M, Zhang X, Zhao Q, Kochanek PM, Kagan VE. Mass-spectrometric characterization of phospholipids and their primary peroxidation products in rat cortical neurons during staurosporine-induced apoptosis. J Neurochem. 2008; 107:1614–1633. [PubMed: 19014376]
46. Tyurin VA, Tyurina YY, Ritov VB, Lysytsya A, Amoscato AA, Kochanek PM, Hamilton R, Dekosky ST, Greenberger JS, Kagan VE. Oxidative lipidomics of apoptosis: quantitative assessment of phospholipid hydroperoxides in cells and tissues. Methods Mol Biol. 2010; 610:353–374. [PubMed: 20013189]
47. Tyurin VA, Tyurina YY, Jung MY, Tungekar MA, Wasserloos KJ, Bayir H, Greenberger JS, Kochanek PM, Shvedova AA, Kagan VE. Mass-spectrometric analysis of hydroperoxy- and hydroxy-derivatives of cardiolipin and phosphatidylserine in cells and tissues induced by pro-apoptotic and pro-inflammatory stimuli. J Chromatogr B Anal Technol Biomed Life Sci. 2009; 877:2863–2872.
48. Tyurina YY, Tyurin VA, Kaynar AM, Kapralova VI, Wasserloos KJ, Li J, Mosher M, Wright L, Wipf P, Kagan VE. Oxidative lipidomics of hyperoxic acute lung injury: Mass spectrometric characterization of cardiolipin and phosphatidylserine peroxidation. Am J Physiol Lung Cell Mol Physiol. 2010; 299:L73–L85. [PubMed: 20418384]

49. Rouser G, Fkeischer S, Yamamoto A. Two dimensional then layer chromatographic separation of polar lipids and determination of phospholipids by phosphorus analysis of spots. Lipids. 1970; 5:494–496. [PubMed: 5483450]
50. Holmes AJ, Williams DLH. Reaction of S-nitrosothiols with ascorbate: clear evidence of two reactions. Chem Commun. 1998:1711–1712.
51. Wang X, Tanus-Santos JE, Reiter CD, Dejam A, Shiva S, Smith RD, Hogg N, Gladwin MT. Biological activity of nitric oxide in the plasmatic compartment. Proc Natl Acad Sci USA. 2004; 101:11477–11482. [PubMed: 15258287]
52. Hu Z, Chandran K, Grasso D, Smets BF. Nitrification inhibition by ethylenediamine-based chelating agents. Environ Eng Sci. 20:222–228.
53. Bottcher CJF, Van Gent CM, Fries C. A rapid and sensitive sub-micro phosphorus determination. Anal Chim Acta. 1961; 24:203–204.
54. Hsu FF, Turk J, Rhoades ER, Russell DG, Shi Y, Groisman EA. Structural characterization of cardiolipin by tandem quadrupole and multiple-stage quadrupole ion-trap mass spectrometry with electrospray ionization. J Am Soc Mass Spectrom. 2005; 16:491–504. [PubMed: 15792718]
55. Pena LA, Fuks Z, Kolesnick RN. Radiation-induced apoptosis of endothelial cells in the murine central nervous system: protection by fibroblast growth factor and sphingomyelinase deficiency. Cancer Res. 2000; 60:321–327. [PubMed: 10667583]
56. Fei P, El-Deiry WS. P53 and radiation responses. Oncogene. 2003; 22:5774–5783. [PubMed: 12947385]
57. Eliopoulos AG, Kerr DJ, Herod J, Hodgkins L, Krajewski S, Reed JC, Young LS. The control of apoptosis and drug resistance in ovarian cancer: influence of p53 and Bcl-2. Oncogene. 1995; 11:1217–1228. [PubMed: 7478541]
58. Miyashita T, Reed JC. Tumor suppressor p53 is a direct transcriptional activator of the human bax gene. Cell. 1995; 80:293–299. [PubMed: 7834749]
59. Basu S, Bayoumy S, Zhang Y, Lozano J, Kolesnick R. BAD enables ceramide to signal apoptosis via Ras and Raf-1. J Biol Chem. 1998; 273:30419–30426. [PubMed: 9804808]
60. Aird WC. Phenotypic heterogeneity of the endothelium: II. Representative vascular beds. Circ Res. 2007; 100:174–190. [PubMed: 17272819]
61. Ochoa CD, Wu SS, Stevens T. New developments in lung endothelial heterogeneity: von Willebrand factor, P-selectin and the Weibel-Palade body. Semin Thromb Hemostas. 2010; 36:301–308.
62. Kuebler WM, Parthasarathi K, Lindert J, Bhattacharya J. Real-time lung microscopy. J Appl Physiol. 2007; 102:1255–1264. [PubMed: 17095639]
63. Huh D, Matthews BD, Mammoto A, Montoya-Zavala M, Hsin HY, Ingber DE. Reconstituting organ-level lung functions on a chip. Science. 2010; 328:1662–1668. [PubMed: 20576885]
64. Iwase H, Takatori T, Niijima H, Nagao M, Amano T, Iwadate K, Matsuda Y, Nakajima M, Kobayashi M. Formation of leukotoxin (9,10-epoxy-12-octadecenoic acid) during the autoxidation of phospholipids promoted by hemoproteins. Biochim Biophys Acta. 1997; 1345:27–34. [PubMed: 9084498]
65. Iwase H, Takatori T, Nagao M, Nijima H, Iwadate K, Matsuda Y, Kobayashi M. Formation of keto and hydroxy compounds of linoleic acid in submitochondrial particles of bovine heart. Free Radic Biol Med. 1998; 24:1492–1503. [PubMed: 9641268]
66. Bronstein JC, Bull AW. Substrate specificity and characterization of partially purified rat liver 13-hydroxyoctadecadienoic acid (13-HODE) dehydrogenase. Arch Biochem Biophys. 1997; 348:219–225. [PubMed: 9390194]
67. Hamm H, Kroegel C, Hohlfeld J. Surfactant: A review of its functions and relevance in adult respiratory disorders. Respir Med. 1996; 90:251–270. [PubMed: 9499810]
68. Schmidt R, Meier U, Yabut-Perez M, Walmrath D, Grimminger F, Seeger W, Gunther A. Alteration of fatty acid profiles in different pulmonary surfactant phospholipids in acute respiratory distress syndrome and severe pneumonia. Am J Respir Crit Care Med. 2001; 163:95–100. [PubMed: 11208632]

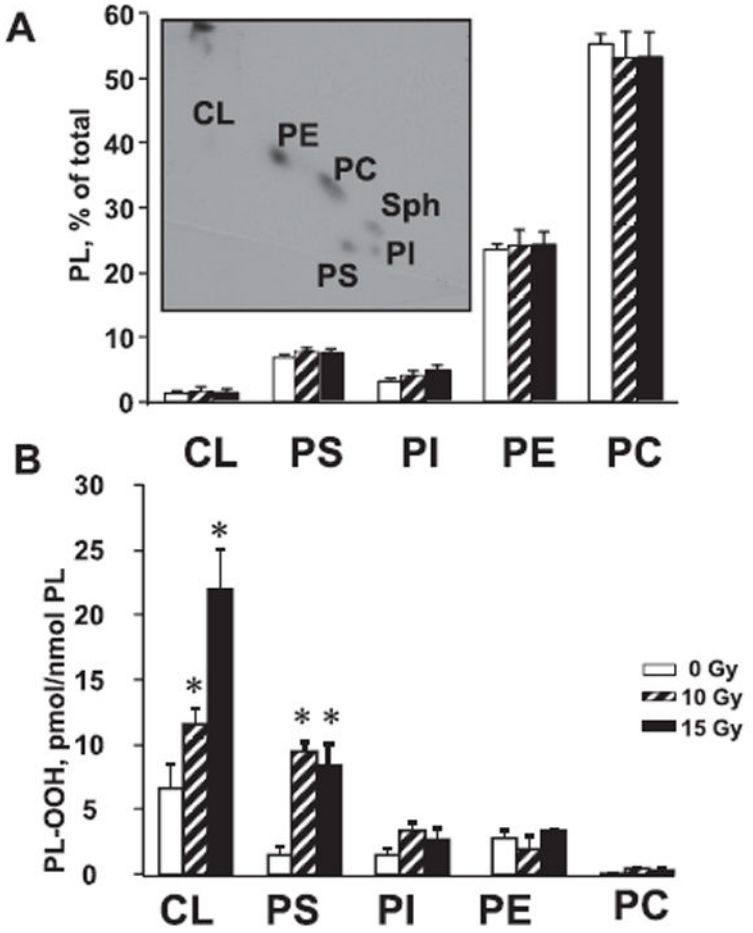

FIG. 1.

Phospholipid composition and accumulation of phospholipid hydroperoxides in lungs of mice after TBI. Panel A: Phospholipid composition of control and irradiated lung. Mice were irradiated with 10 and 15 Gy. Inset: Typical 2D-HPTLC chromatogram of total lipids extracted from control mouse lung. Panel B: Accumulation of PL-OOH in lung of mice irradiated with 10 and 15 Gy. Data are means ± SD; $n = 4$ for control; $n = 3$ for TBI. *$P <$ 0.05 compared to control nonirradiated mice. CL, cardiolipin; PE, phosphatidylethanolamine; PC, phosphatidylcholine; PI, phosphatidylinositol; PS, phosphatidylserine.

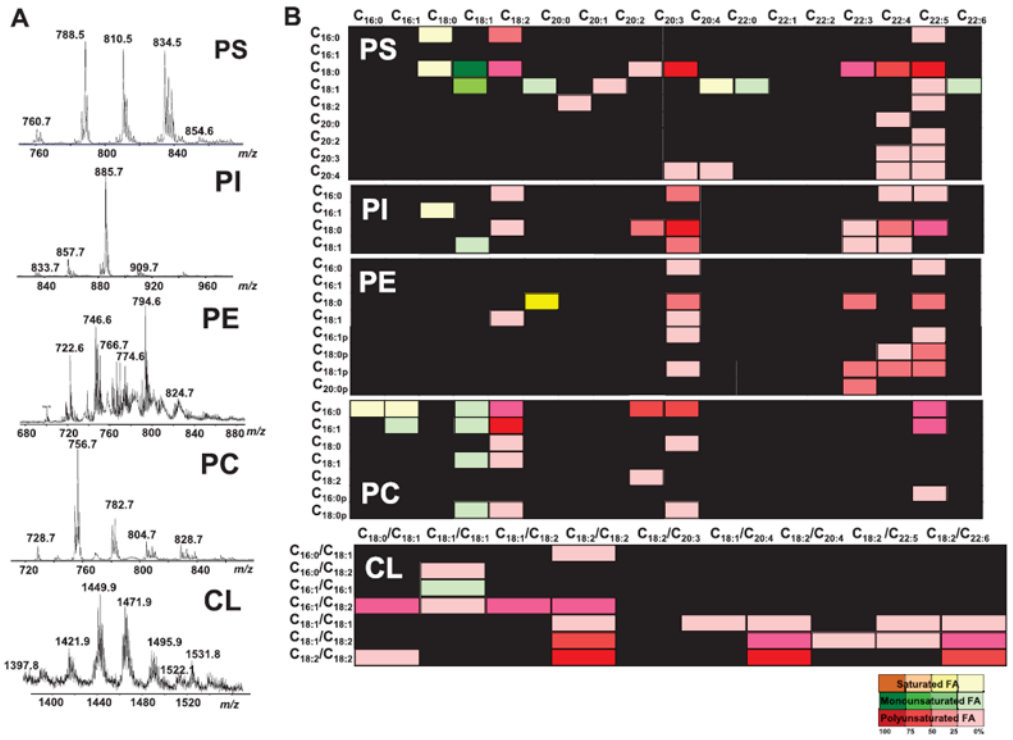

FIG. 2.

Identification of major phospholipid classes in mouse lung by ESI-MS. Panel A: Typical mass spectra of phospholipids isolated from mouse lung. Panel B: A lipid profile map of mouse lung. Fatty acids residues of phospholipids are shown as columns (on the left) and lines (on the top) of each of phospholipids; individual molecular species are identifiable as a colored square at the intersection of the respective columns and lines. For CL with four fatty acid residues, paired combinations of two fatty acids are shown. The intensity of the colors corresponds to the abundance of a given molecular species. CL, cardiolipin; PE, phosphatidylethanolamine; PC, phosphatidylcholine; PI, phosphatidylinositol; PS, phosphatidylserine; FA, fatty acids.

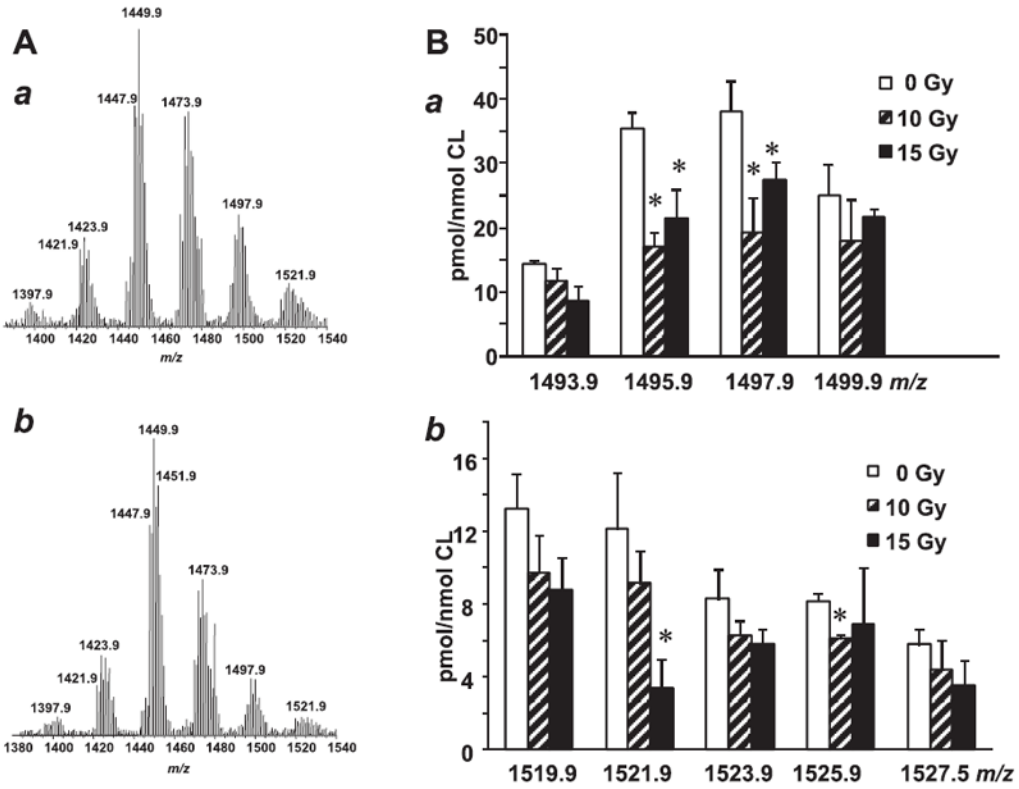

FIG. 3.

Radiation-induced oxidation of CL in mouse lung. Panel A: Typical full negative LC/ESI-MS spectrum of CL isolated from control mouse lung (a) and the lung of mice after TBI at a dose of 15 Gy (b). Panel B: Quantitative assessment of CL molecular species with *m/z* in the range from 1493.9 to 1499.9 (a) and *m/z* in the range from 1519.9 to 1527.9 (b) in control lung and lung isolated from mice after TBI. Data are means ± SD; $n = 4$ for control; $n = 3$ for TBI. *$P < 0.05$ compared to nonirradiated mice.

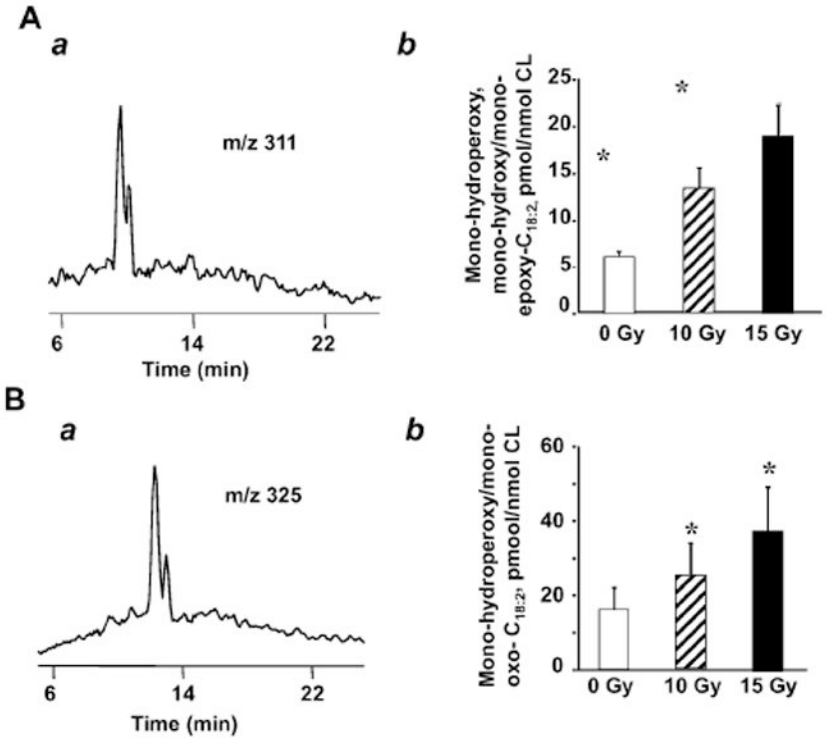

FIG. 4.

Quantitative assessment and identification of oxygenated fatty acids in CL obtained from lungs of mice after TBI. Panel A: Base peak of oxygenated $C_{18:2}$ with *m/z* 311 (a) and quantitative assessment of oxygenated $C_{18:2}$ in CL isolated from control lungs and lungs of mice after TBI (b). Data are means ± SD; $n = 4$ for control; $n = 3$ for TBI, $^*P < 0.05$ compared to control nonirradiated mice. Panel B: Base peak of oxygenated $C_{18:2}$ with *m/z* 325 (a) and quantitative assessment of oxygenated $C_{18:2}$ in CL isolated from the control lungs and lungs of mice after TBI (b). Open bars, control; gray closed bars, TBI at 10 Gy; black closed bars, TBI at 15 Gy. Data are means ± SD; $n = 4$ for control; $n = 3$ for TBI. $^*P < 0.05$ compared to control nonirradiated mice.

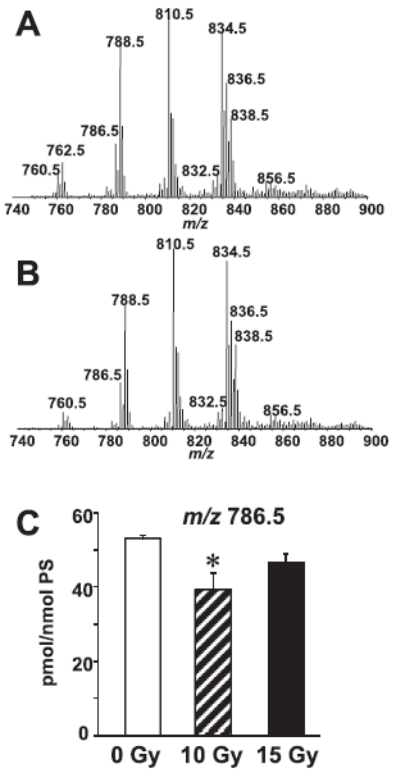

FIG. 5.

Oxidation of PS in lung of mice exposed to TBI. Panel A: Typical full negative LC/ESI-MS spectrum of PS isolated from a control mouse lung. Panel B: Typical full negative LC/ESI-MS spectrum of PS isolated from irradiated mouse lung. A decrease in the intensity of molecular ions with *m/z* 786.5 ($C_{18:0}/C_{18:2}$) in irradiated lung was detected. Panel C: Quantitative assessment of PS molecular species in control and irradiated lung. Data are means ± SD; $n = 4$ for control; $n = 3$ for TBI. *$P < 0.05$ compared to control nonirradiated mice.

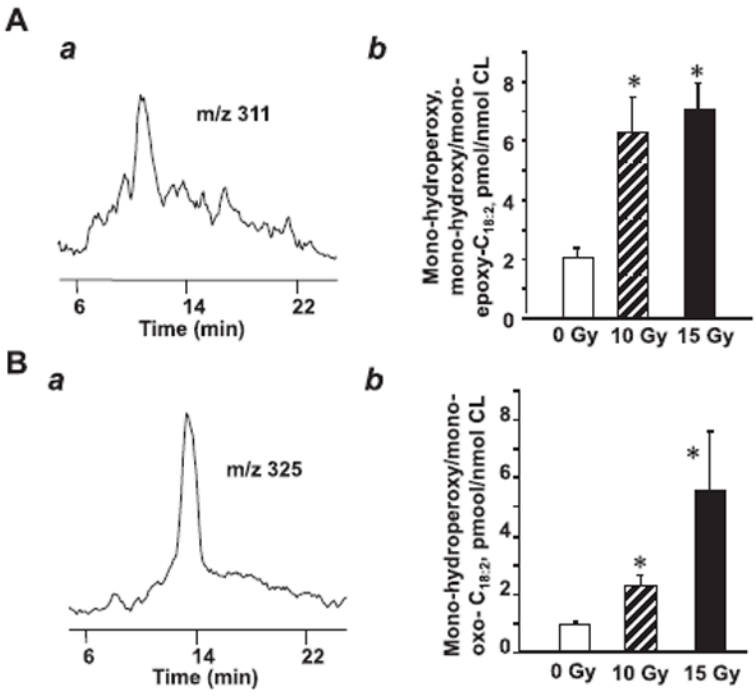

FIG. 6.

Accumulation of oxygenated linoleic acid ($C_{18:2}$) in PS from lungs of mice after TBI. Panel A: Typical base peak (a) and quantitative assessment of molecular ion with *m/z* 311 obtained from lungs of control and irradiated mice (b). Panel B: Typical base peak (a) and quantitative assessment of molecular ion with *m/z* 325 obtained from lungs of control and irradiated mice (b). Data are means ± SD; $n = 4$ for control; $n = 3$ for TBI. $^*P < 0.05$ compared to control nonirradiated mice.

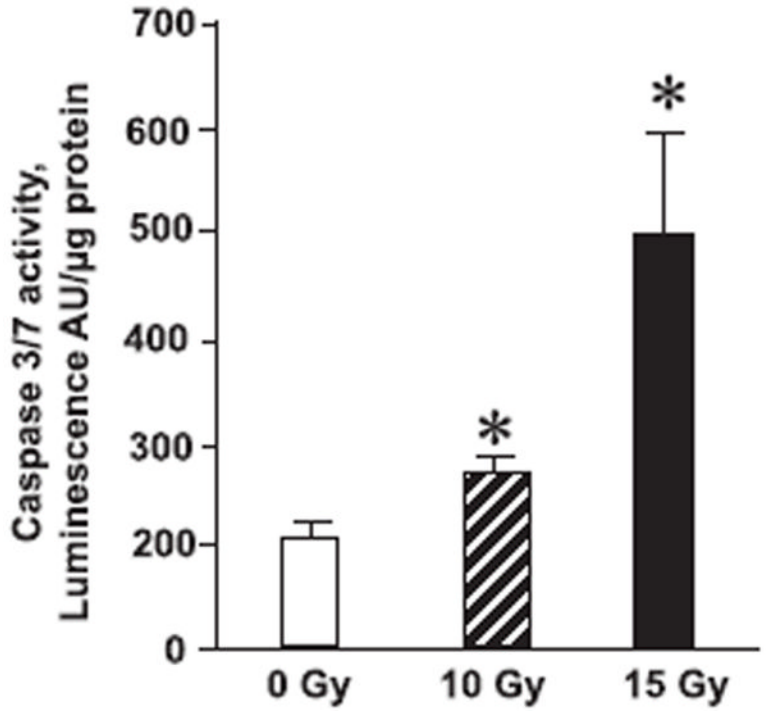

FIG. 7.

Caspase 3/7 activity in mouse lung. Activity of caspase 3/7 was significantly increased in lungs of mice after TBI. Data are means ± SD; $n = 4$ for control; $n = 3$ for TBI. *$P < 0.05$ compared to control non irradiated mice.

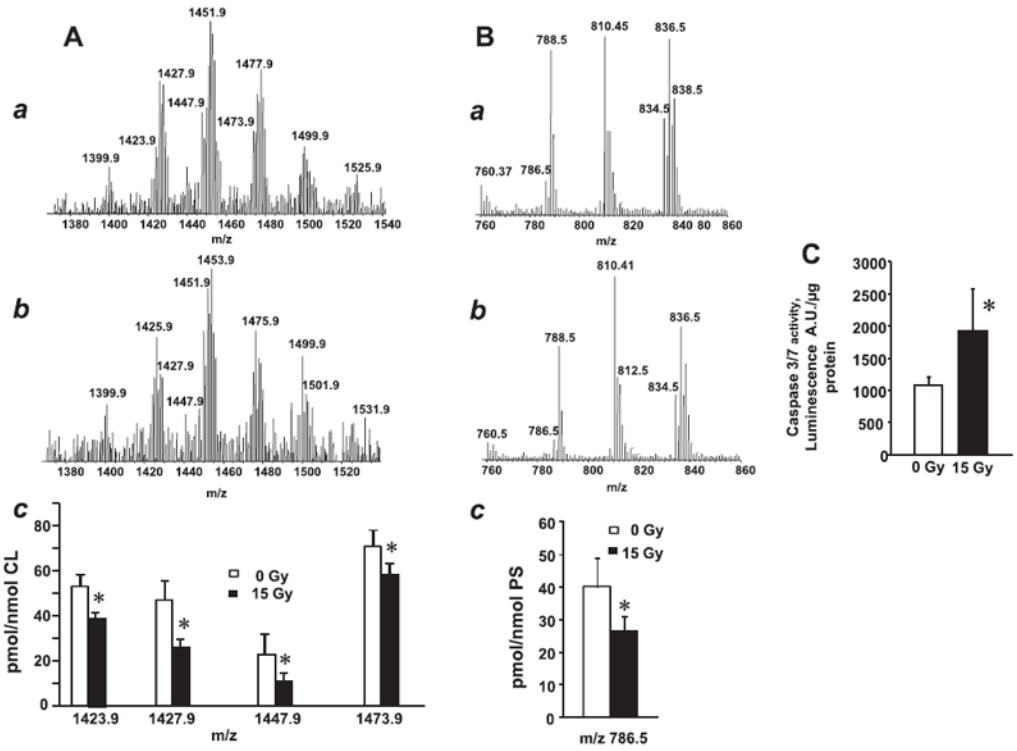

FIG. 8.

Gamma-radiation-induced oxidation of CL and PS and apoptosis in mouse lung endothelial cells. Panel A: Typical negative LC/ESI-MS spectra of CL obtained from control cells (a) and cells 48 h after γ irradiation (15 Gy) (b). Panel B: Typical negative LC/ESI-MS spectra of PS obtained from control cells (a) and cells 48 h after γ irradiation (15 Gy) (b). Quantitative assessment of LC and PS molecular species (c). Panel C: Caspase 3/7 activity in mouse lung endothelial cells. Open bars, control; black closed bars, 48 h after γ irradiation (15 Gy). Data are means ± SD; $n = 3$. *$P < 0.05$ compared to nonirradiated cells.